

THERMIONIC AND ADSORPTION CHARACTERISTICS OF A SINGLE-
CRYSTAL TUNGSTEN FILAMENT EXPOSED TO OXYGEN

by

WERNER ENGELMAIER

Ing., Technologisches Gewerbemuseum
Vienna, Austria
(1958)

S.B., University of South Carolina
(1965)

SUBMITTED IN PARTIAL FULFILLMENT
OF THE REQUIREMENTS FOR THE
DEGREE OF MASTER OF SCIENCE

at the

MASSACHUSETTS INSTITUTE OF TECHNOLOGY

June, 1966

Signature of Author.....
Department of Mechanical Engineering, May 20, 1966

Certified by.....
Thesis Supervisor

Accepted by.....
Chairman, Departmental Committee
on Graduate Students

THERMIONIC AND ADSORPTION CHARACTERISTICS OF A SINGLE-
CRYSTAL TUNGSTEN FILAMENT EXPOSED TO OXYGEN

by

Werner Engelmaier

Submitted to the Department of Mechanical Engineering
on May 20, 1966 in partial fulfillment of the require-
ments for the degree of Master of Science.

ABSTRACT

Measurement of the thermionic current emitted in the various crystallographic directions of a single-crystal tungsten filament were used to determine the changes in the vacuum work functions resulting from prolonged exposure to oxygen, the dependence of the work functions of different crystallographic directions on oxygen pressure and filament temperature, and the desorption energy of oxygen on tungsten. As an attempt to remove carbon impurities from tungsten, the filament was held at 2200°K for 63 hours in oxygen at a pressure of 1×10^{-6} Torr. Subsequent emission measurements indicate that this process did not produce significant changes in the vacuum work function. The effective work functions of the (100), (111), (112), and (110) crystallographic directions were determined for filament temperatures of 1900°K to 2200°K and oxygen pressures of 1×10^{-9} to 5×10^{-6} Torr. Since oxygen migrates rapidly over the filament surface at the high temperatures employed here, it was not possible to determine the dependence of the oxygen desorption energy on the crystallographic direction of the substrate. The apparent desorption energy was essentially the same for the various directions, the average value being 5.9 eV.

Thesis Supervisor: Robert E. Stickney

Title: Assistant Professor of Mechanical Engineering

ACKNOWLEDGEMENTS

I would like to express my deep gratitude to Professor Robert E. Stickney for his suggestion of this problem and for his guidance and encouragement throughout this work. The previous study by Mr. James L. Coggins was of invaluable help, since I was able to use a substantial part of his apparatus for my work. The assistance and advice that Mr. Lawrence E. Sprague gave me during the course of this research was extremely helpful.

I would like to acknowledge the technical support received from the M.I.T. Research Laboratory of Electronics; particularly to Messrs. John B. Keefe, Walter Reimann, and Robert M. DiGiacomo who provided the necessary skills for the construction of my apparatus. Much time was saved through the computational support given by the M.I.T. Computation Center. I wish to express my appreciation to Mrs. Rose Hurvitz for typing the manuscript.

I further would like to express my deep gratitude to my wife, Osie, who contributed very much to this study through her constant cheerful encouragement and patient endurance.

This research was supported by the National Aeronautics and Space Administration (Grant NGR-22-009-091).

TABLE OF CONTENTS

	<u>Page</u>
ABSTRACT	2
ACKNOWLEDGEMENTS	3
LIST OF FIGURES	5
I. INTRODUCTION	6
II. APPARATUS	6
III. RESULTS: VACUUM MEASUREMENTS AND OXYGEN TREATMENT	13
IV. RESULTS: DEPENDENCE OF WORK FUNCTION ON OXYGEN PRESSURE	13
V. RESULTS: DESORPTION ENERGY FOR O ₂ ON W	28
VI. DISCUSSION OF RESULTS	33
REFERENCES	36

LIST OF FIGURES

	<u>Page</u>
Fig. 1 Schematic diagram of tube.	7
Fig. 2 Schematic diagram of system.	8
Fig. 3 Richardson plots for the (100) crystallographic direction in vacuum.	10
Fig. 4 Richardson plots for the (111) crystallographic direction in vacuum.	11
Fig. 5 Emission maps for 1900°K in vacuum.	12
Fig. 6 Emission maps for an O ₂ pressure of 1x10 ⁻⁸ Torr.	14
Fig. 7 Emission maps for an O ₂ pressure of 1x10 ⁻⁷ Torr.	15
Fig. 8 Emission maps for an O ₂ pressure of 1.2x10 ⁻⁶ Torr.	16
Fig. 9a Effective work function of the (100) crystallographic direction as a function of O ₂ pressure and filament temperature.	18
Fig. 9b Effective work function of the (111) crystallographic direction as a function of O ₂ pressure and filament temperature.	19
Fig. 9c Effective work function of the (112) crystallographic direction as a function of O ₂ pressure and filament temperature.	20
Fig. 9d Effective work function of the (110) crystallographic direction as a function of O ₂ pressure and filament temperature.	21
Fig. 10a Effective work function of the (100) crystallographic direction as a function of T/T _R [*] .	23
Fig. 10b Effective work function of the (111) crystallographic direction as a function of T/T _R [*] .	24
Fig. 10c Effective work function of the (112) crystallographic direction as a function of T/T _R [*] .	25
Fig. 10d Effective work function of the (110) crystallographic direction as a function of T/T _R [*] .	26
Fig. 11 Comparison of the average experimental results for O ₂ on W; ϕ_E vs T/T _R [*] for the (100), (111), (112), and (110) crystallographic directions.	27
Fig. 12 Typical data obtained in desorption study.	29

I. INTRODUCTION

Over forty years ago, Langmuir and Kingdon¹ observed that the thermionic emission from a cesiated tungsten filament could be increased markedly by adsorbing O_2 upon the filament. Although this problem has received very little attention in subsequent years, it is currently being reconsidered because of its possible importance to thermionic energy conversion.² In the past five years there have been an increasing number of investigations of the effects of electronegative gases (such as O_2 and F_2) on the thermionic properties of cesiated refractory metals.³

Since we cannot expect to understand fully the properties of $Cs + O_2$ systems until the properties of Cs and O_2 systems are determined separately, the present experiment is designed to study the thermionic and adsorption characteristics of a single-crystal tungsten filament exposed to pure O_2 . Results are reported for the dependence of work function on crystallographic direction, filament temperature, and O_2 pressure. In addition, the desorption energy for O_2 on W is determined. Although similar studies have been conducted by others using field emission techniques,^{4,5} the thermionic technique employed here offers the advantage of obtaining data at high filament temperatures over a range of O_2 pressures.

II. APPARATUS

The thermionic tube and circuitry have been described previously by Coggins and Stickney.⁶ The main features of the tube are shown in Fig. 1. Two different tungsten filaments were used during this study because the first one broke before the program was completed. Filament I, having a diameter of 7.2×10^{-3} cm, was used for the emission runs; filament II, having a diameter of 6.88×10^{-3} cm, was used for the remaining

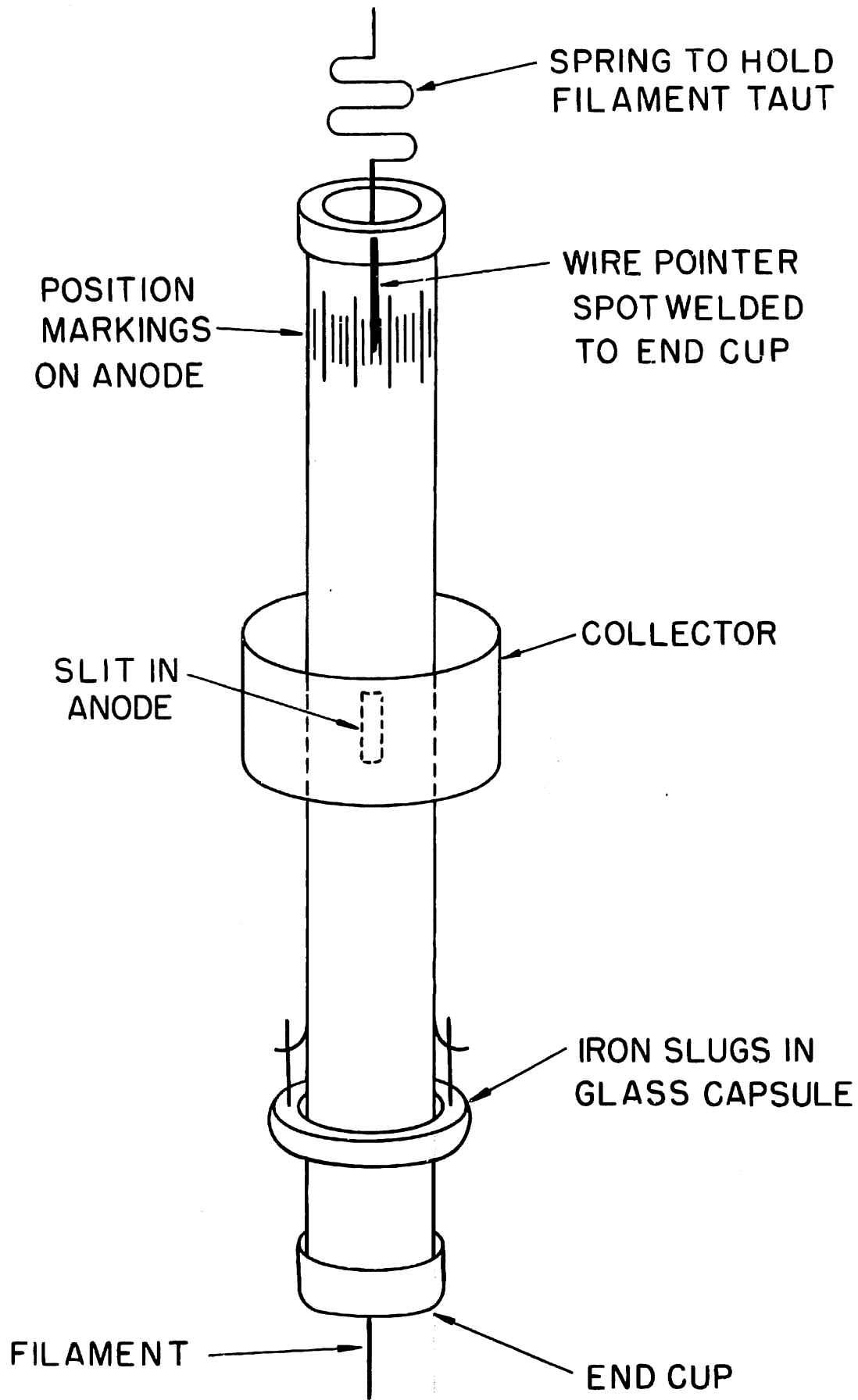


Fig. 1 Schematic diagram of tube.

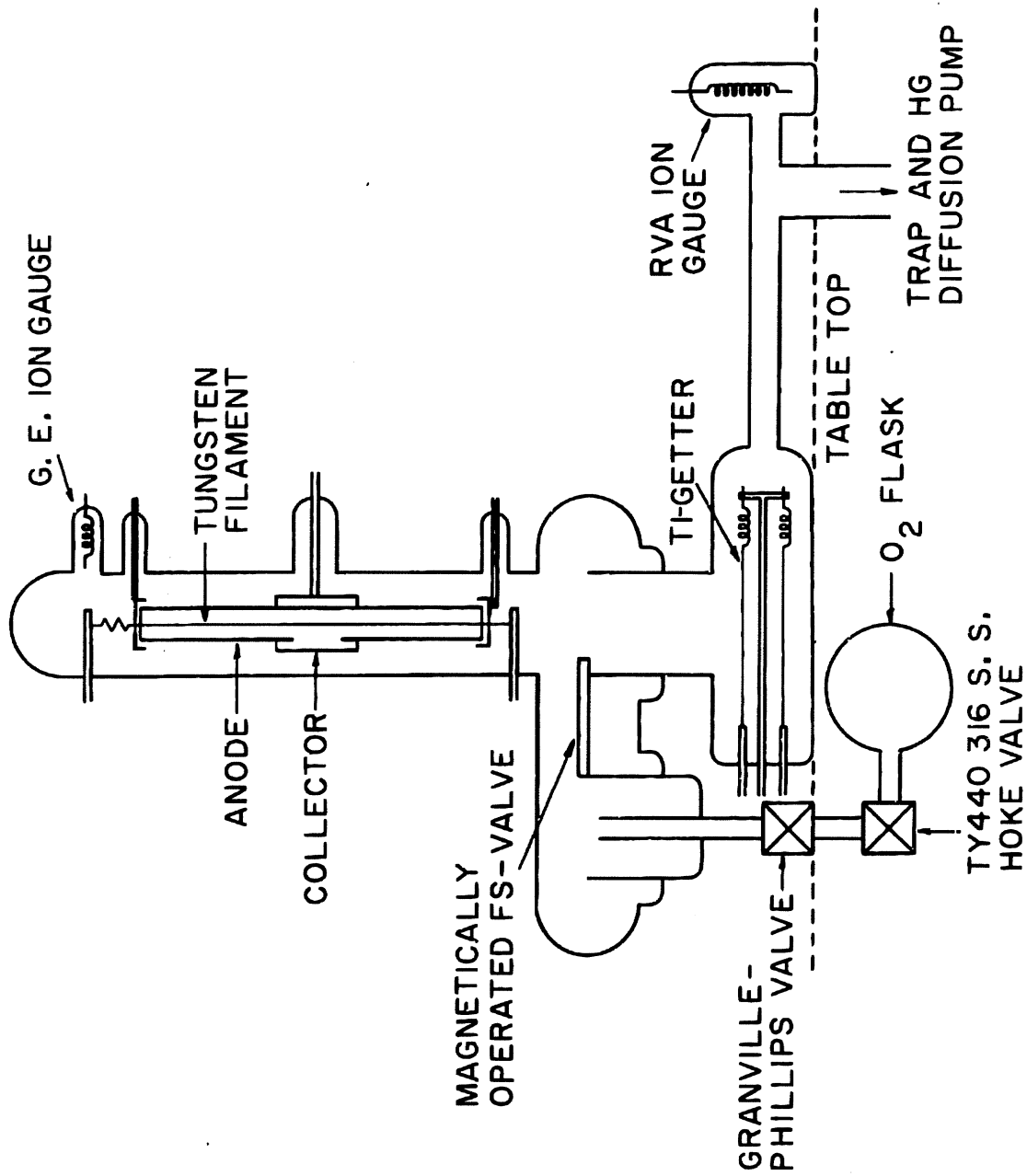


Fig. 2 Schematic diagram of system.

7

experiments. Both filaments were from the same spool of General Electric #218 wire, and they were processed according to the Robinson technique^{7,8} in order to grow a large crystal in the center section. Each crystal was at least 2 cm long and oriented so that the (110) direction was along the axis of the filament.

The anode is a tantalum tube, 2 cm in diameter and 20 cm in length, supported by two end-cups which serve as bearings. Iron slugs enclosed in glass capsules are attached to the anode so that it may be rotated by means of external magnets. A rectangular slit in the anode is aligned parallel to the single crystal in the filament. Since this slit is 0.75 mm wide by 1 cm long, the subtended angle is 4.30° and the corresponding surface area on the filament is $2.70 \times 10^{-4} \text{ cm}^2$ for filament I and $2.58 \times 10^{-4} \text{ cm}^2$ for filament II. By applying a strong electric field between the filament and the anode, the electrons emitted from the filament are accelerated radially and a fraction of these pass through the slit to the collector which is concentric with the anode (Fig. 1). The collector has a diameter of 3 cm and its surface is coated with platinum black in order to reduce electron reflection.⁹ The emission associated with the different crystallographic directions is measured by rotating the anode slit to the appropriate positions.

In the initial part of the experimental program, oxygen from the atmosphere was introduced into the system by diffusion through a heated silver tube. The majority of the program employed, however, the improved system shown schematically in Fig. 2. Here the silver tube has been replaced by a one-liter flask of O_2 and a Granville-Phillips valve for regulating the system pressure. This valve has been equipped with a motor and clutch mechanism so that it may be closed quickly during the desorption tests. A magnetically operated FS (fast sliding) valve is used to control the pumping speed of the system. The titanium getter is employed only for the desorption tests.

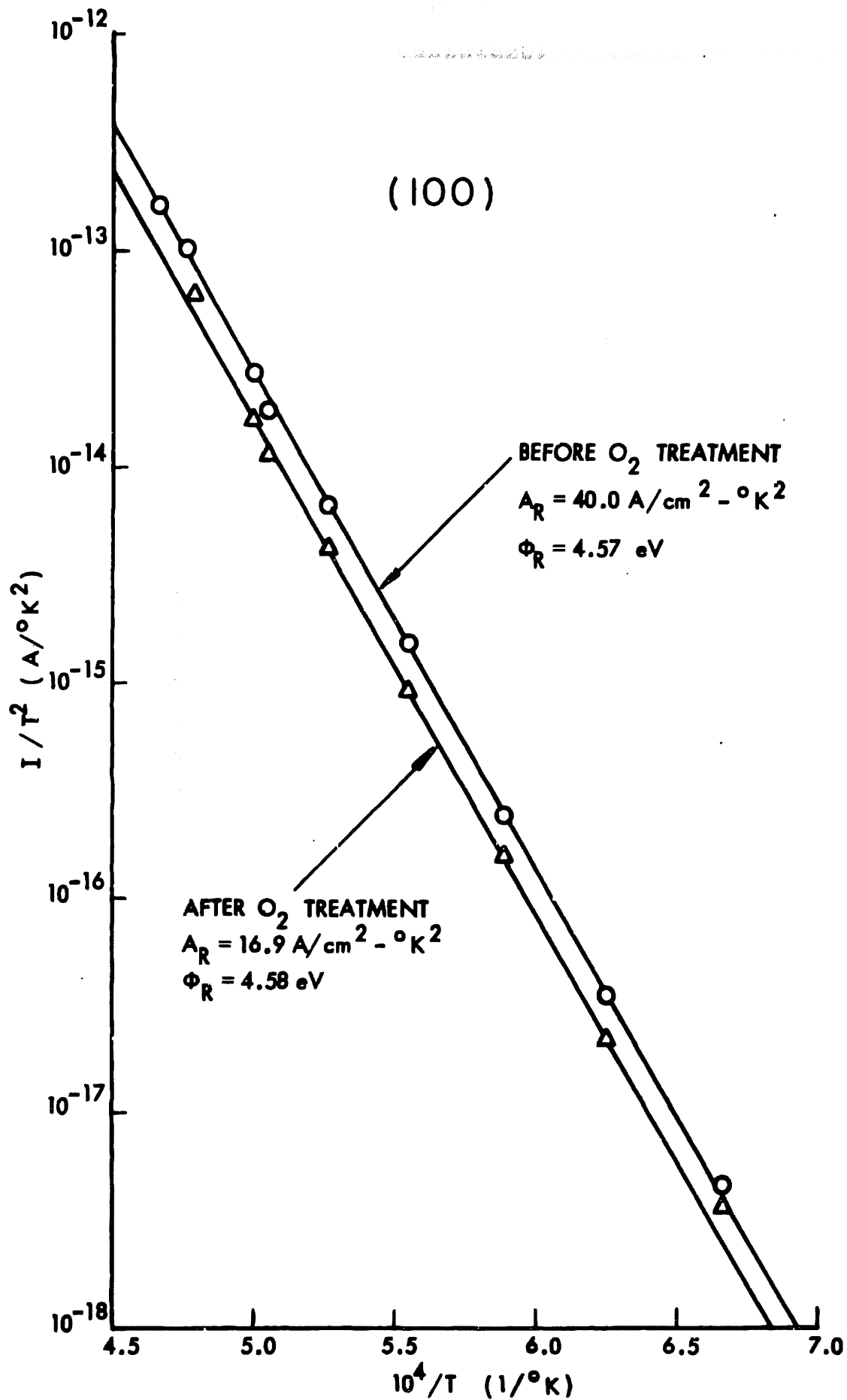


Fig. 3 Richardson plots for the (100) crystallographic direction in vacuum.

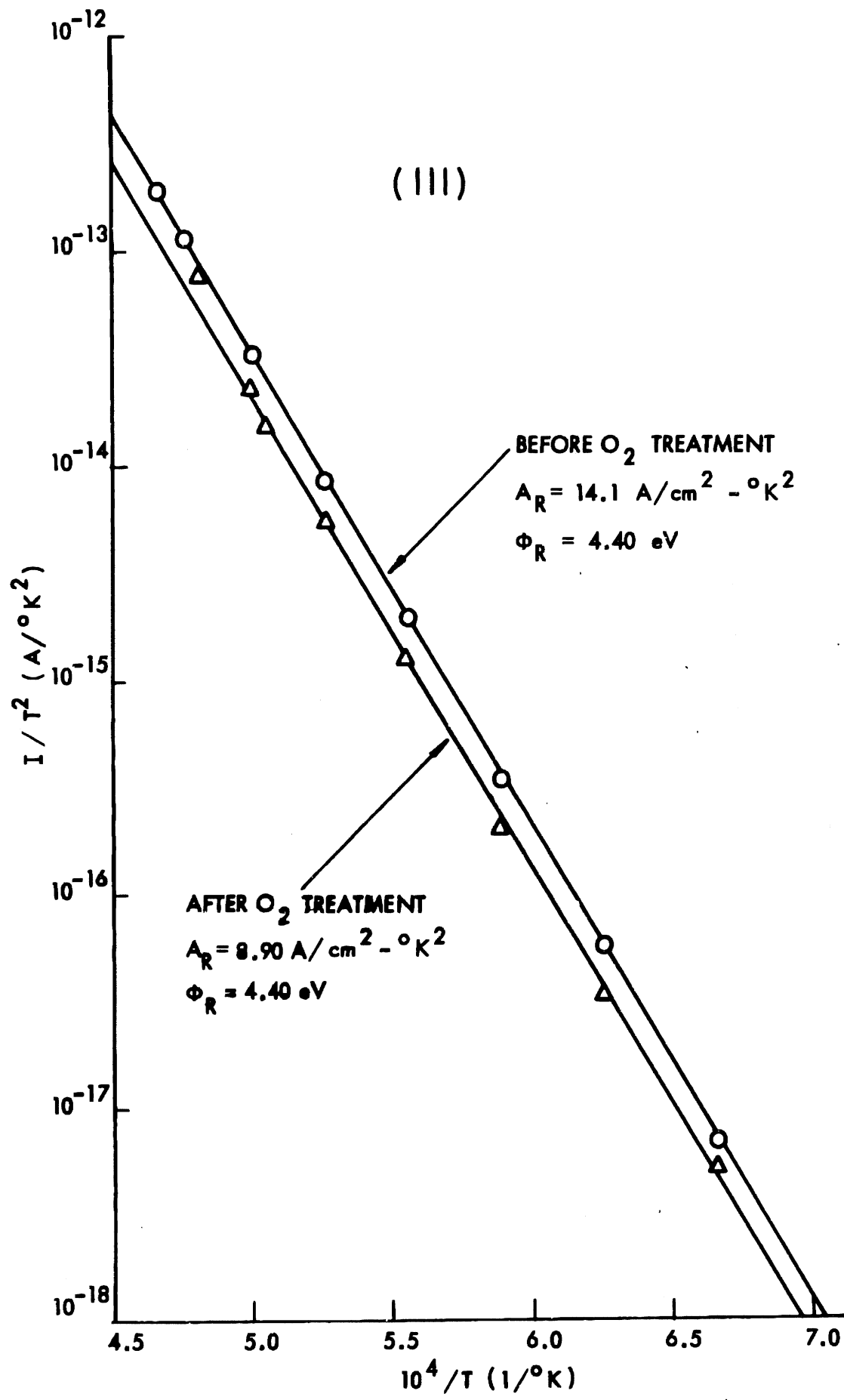


Fig. 4 Richardson plots for the (111) crystallographic direction in vacuum.

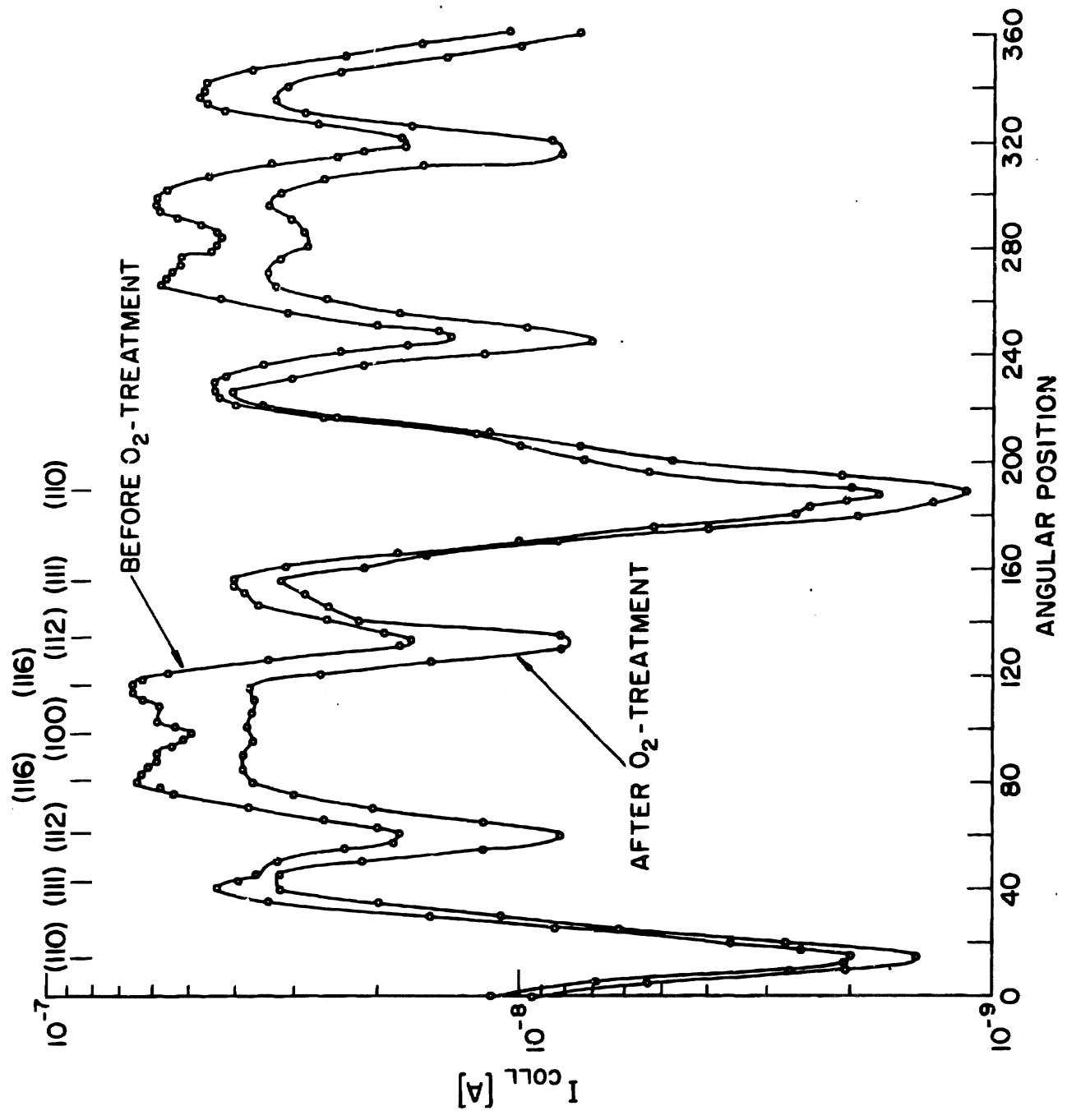


Fig. 5 Emission maps for 1900°K in vacuum.

III. RESULTS: VACUUM MEASUREMENTS AND OXYGEN TREATMENT

Thermionic measurements taken in vacuum ($\sim 3 \times 10^{-10}$ Torr) included Schottky plots, Richardson plots (Figs. 3 and 4), and emission maps (Fig. 5). The Richardson work functions of 4.57 and 4.40 eV obtained for the (100) and (111) directions, respectively, agree well with those reported previously by Nichols,¹⁰ Smith,⁸ Coones,¹¹ and Coggins.¹²

The first test was designed to determine if the thermionic properties of the filament were influenced by the carbon impurities that are generally found to be present in tungsten cathodes. Following the technique recommended by Becker et al.¹³ for removing carbon impurities, the filament was held at 2200°K in oxygen at 1×10^{-6} Torr for 63 hours. After this treatment, the tube was re-evacuated and the Richardson plots shown in Figs. 3 and 4 were obtained. Notice that although the Richardson work functions of the (100) and (111) directions were essentially unchanged, the Richardson constants, A_R , decreased slightly. This decrease in emission is also apparent in the emission maps (Fig. 5). The over-all change is extremely small, and we do not have sufficient evidence to conclude that this change resulted from the removal of carbon impurities alone. These results do indicate, however, that the thermionic properties of the filament are not seriously affected by the oxygen treatment.

IV. RESULTS: DEPENDENCE OF WORK FUNCTION ON OXYGEN PRESSURE

Emission maps taken at various O_2 pressures and filament temperatures are shown in Figs. 6 through 8. As expected, the emission decreases with increasing O_2 pressure. Notice that at the higher pressures the contrast between different crystallographic directions decreases and the (100) direction now emits more strongly than the (116). The last observation, together with the distinct irregularities in the emission maps, may be evidence of rearrangement of the surface structure.¹⁴

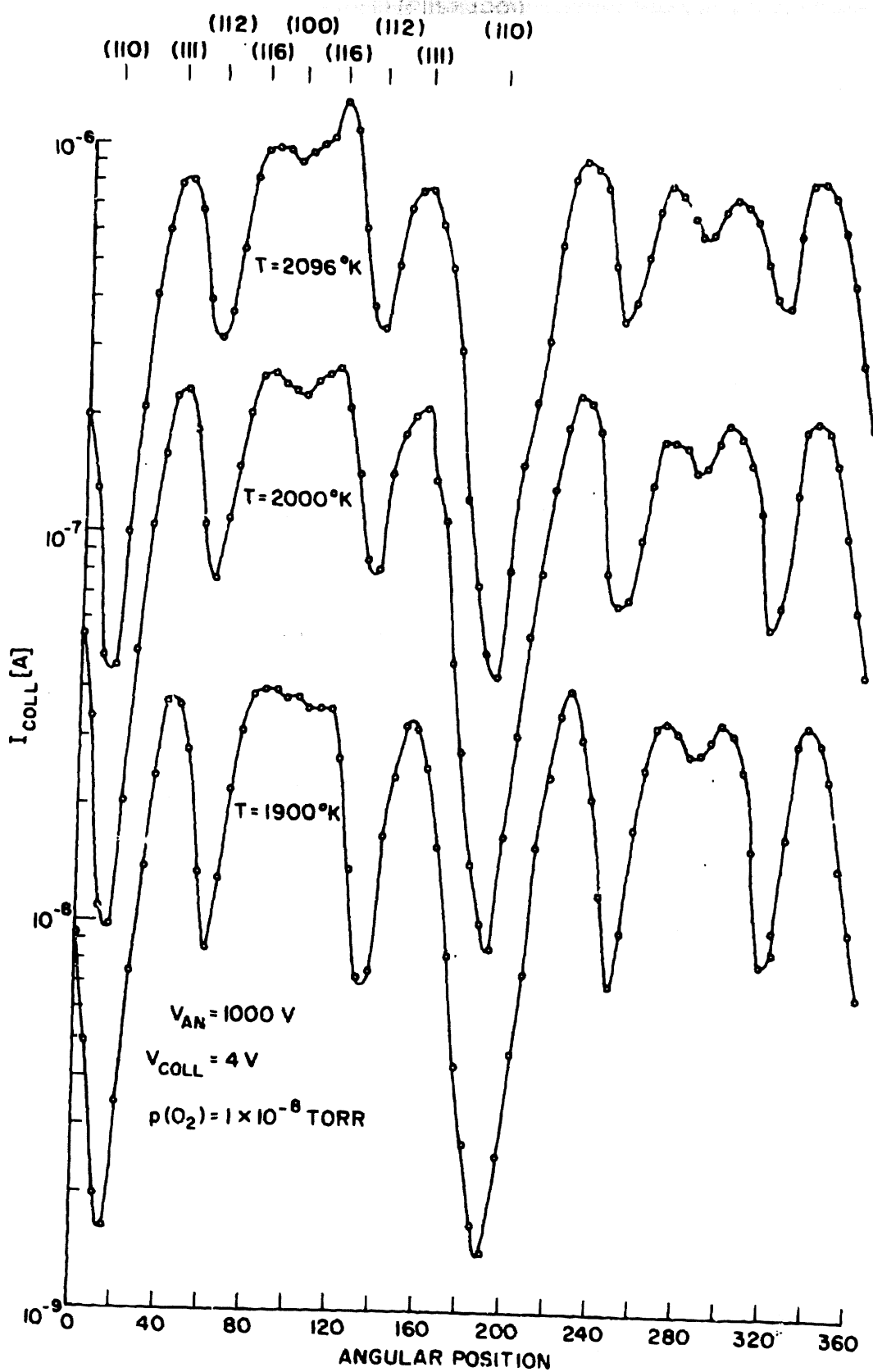


Fig. 6 Emission maps for an O_2 pressure of 1×10^{-8} Torr.

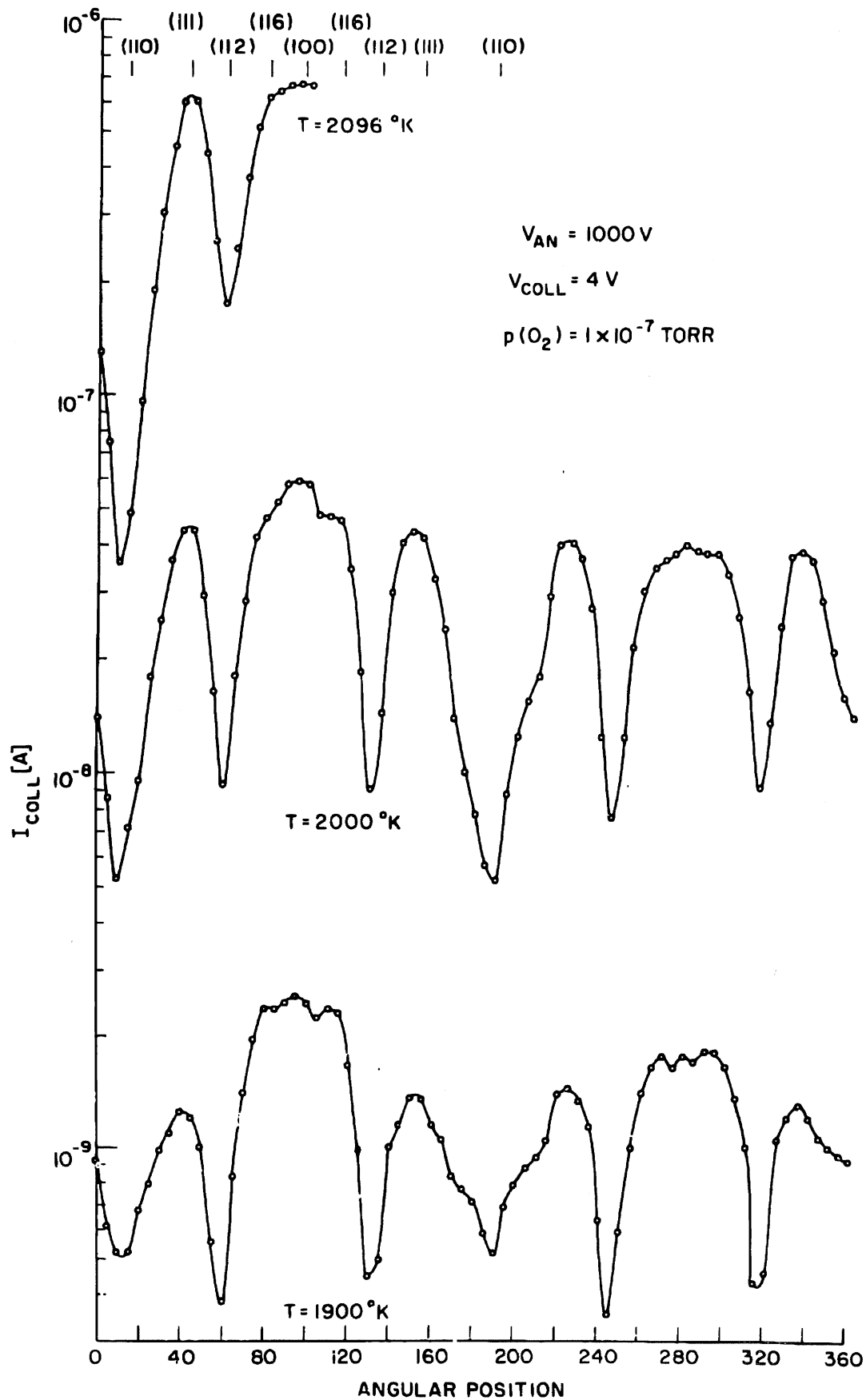


Fig. 7 Emission maps for an O_2 pressure of 1×10^{-7} Torr.

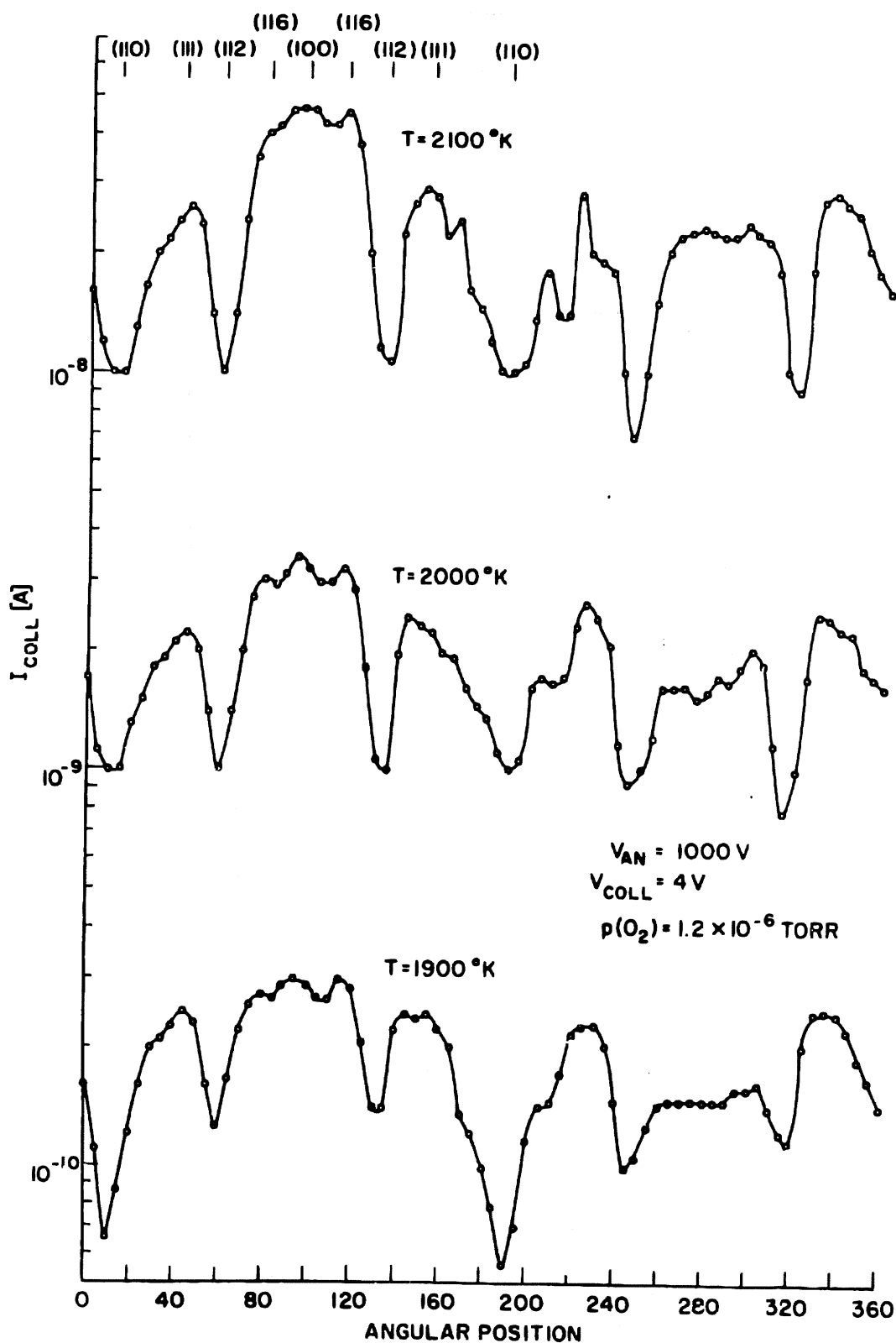


Fig. 8 Emission maps for an O_2 pressure of 1.2×10^{-6} Torr.

At this point in the study filament I broke and was replaced by filament II. At the same time the system was modified by removing the diffusion leak and installing the getter, the FS and GP valves, and the O₂ flask. Since these improvements provide more accurate control of the O₂ pressure, the following data are more reliable than those given in Figs. 6 through 8.

Vacuum measurements indicate that the thermionic properties of the two filaments are almost identical. The results shown in Fig. 9 were obtained by increasing the O₂ pressure in small steps while holding the filament at various temperatures. The effective work function, ϕ_E , is computed from the following form of the Richardson equation,

$$I = 120 ST^2 \exp\left(-\frac{\phi_E}{kT}\right) \quad (1)$$

where I is the measured collector current, S is the filament area subtended by the anode slit, k is Boltzmann's constant, and T is the filament temperature determined from the Jones-Langmuir tables.¹⁵ We have not extrapolated the measurements of I to zero-field conditions because this correction has only a small effect on ϕ_E (~0.05eV) for the anode voltage of 500V employed here.

The pressures reported in Fig. 9 were measured with a General Electric ionization gauge (Model 22GT102). The thoriated iridium filament in the gauge was used to reduce the errors associated with interactions occurring at a hot filament.¹⁶ Since the sensitivity of ionization gauges is not well known for oxygen, we have chosen to express the pressure in terms of the equivalent nitrogen pressure. The true O₂ pressure may differ from the equivalent N₂ pressure by as much as 25 percent. (See Table 5.7 in reference 16.)

The residual gas pressure increases with increasing filament temperature. This fact is illustrated in Fig. 9; the minimum pressure shown for each filament temperature represents

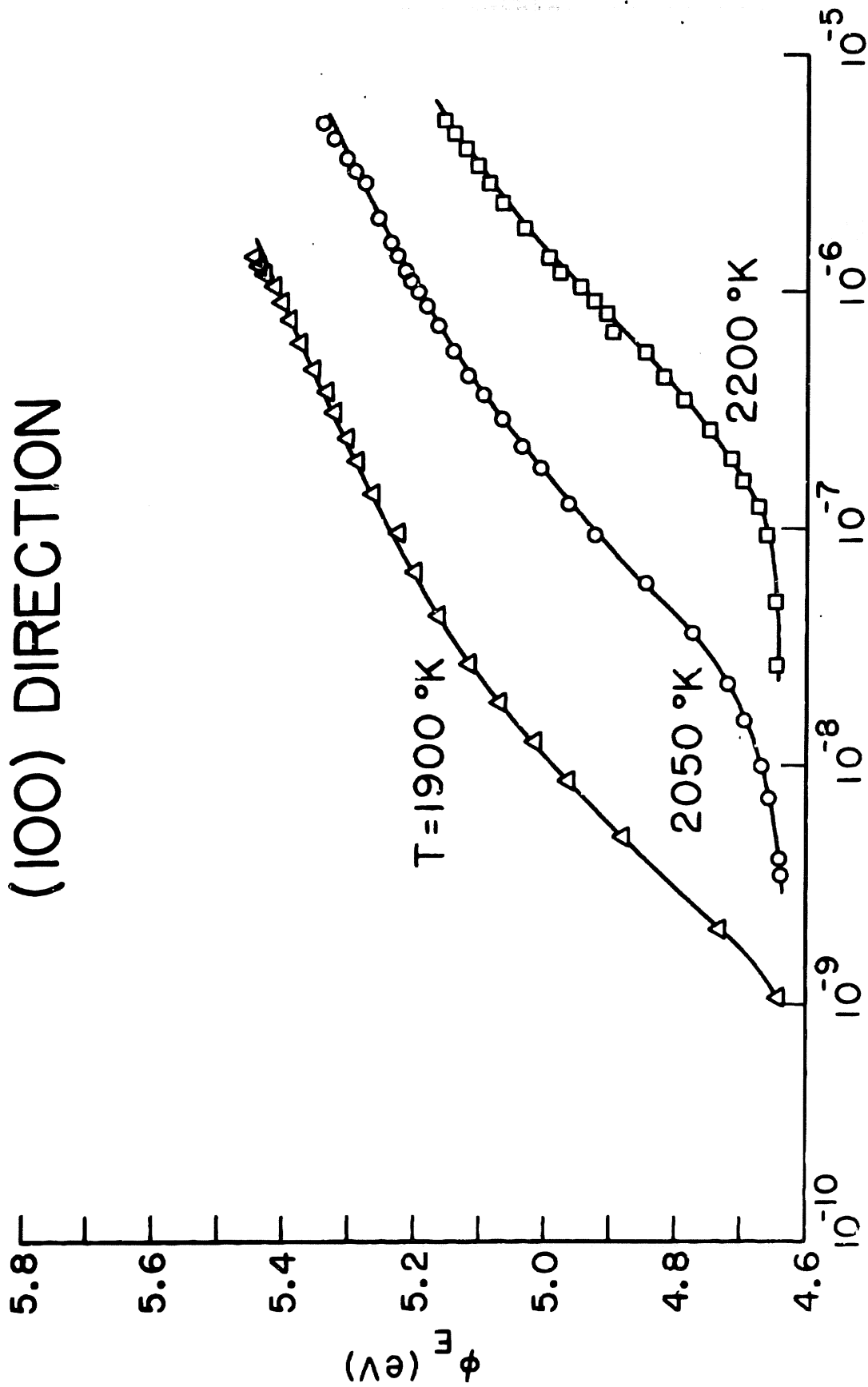
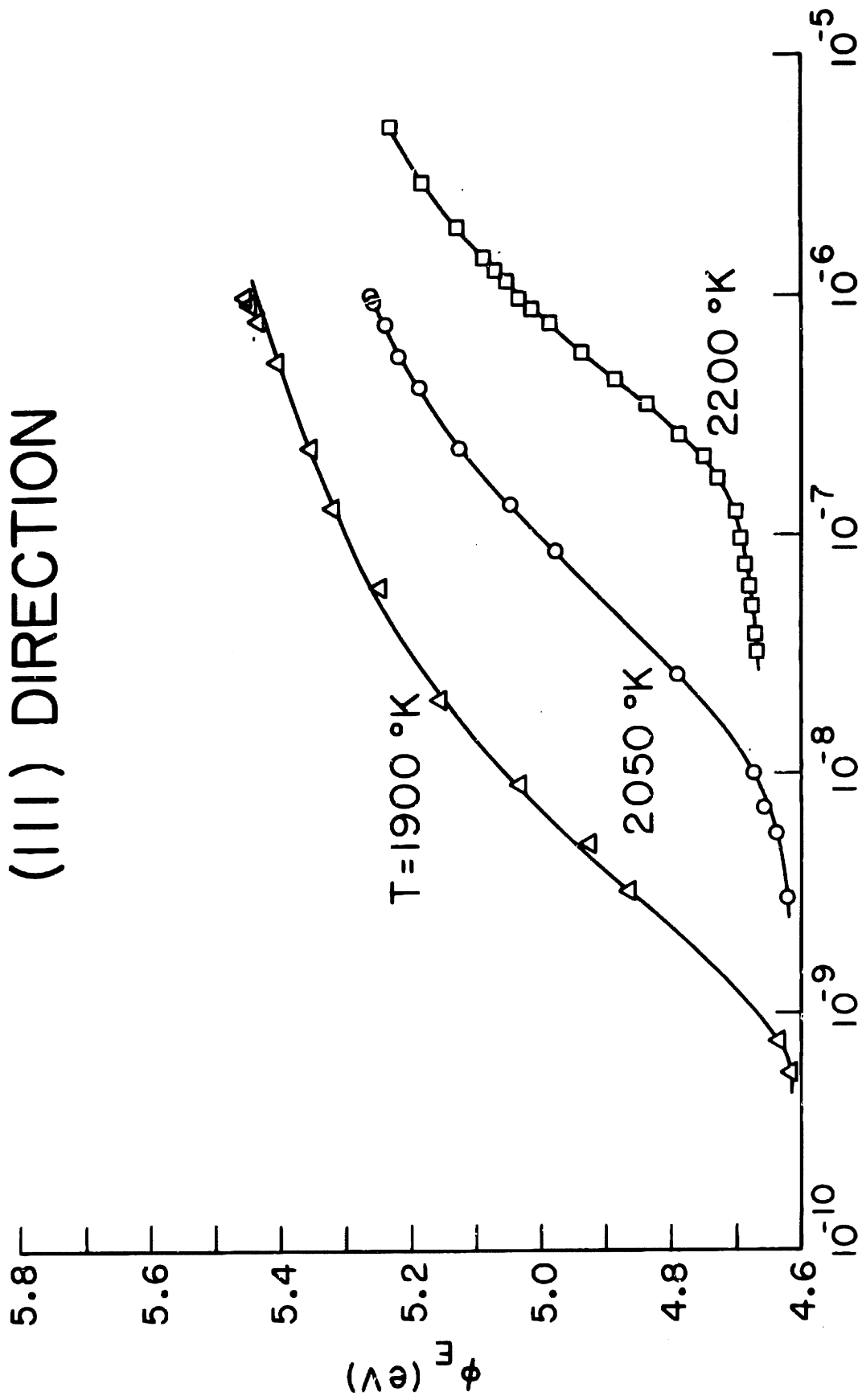


Fig. 9a Effective work function of the (100) crystallographic direction as a function of O_2 pressure and filament temperature.

(111) DIRECTION



PRESSURE (TORR)

Fig. 9b Effective work function of the (111) crystallographic direction as a function of O_2 pressure and filament temperature.

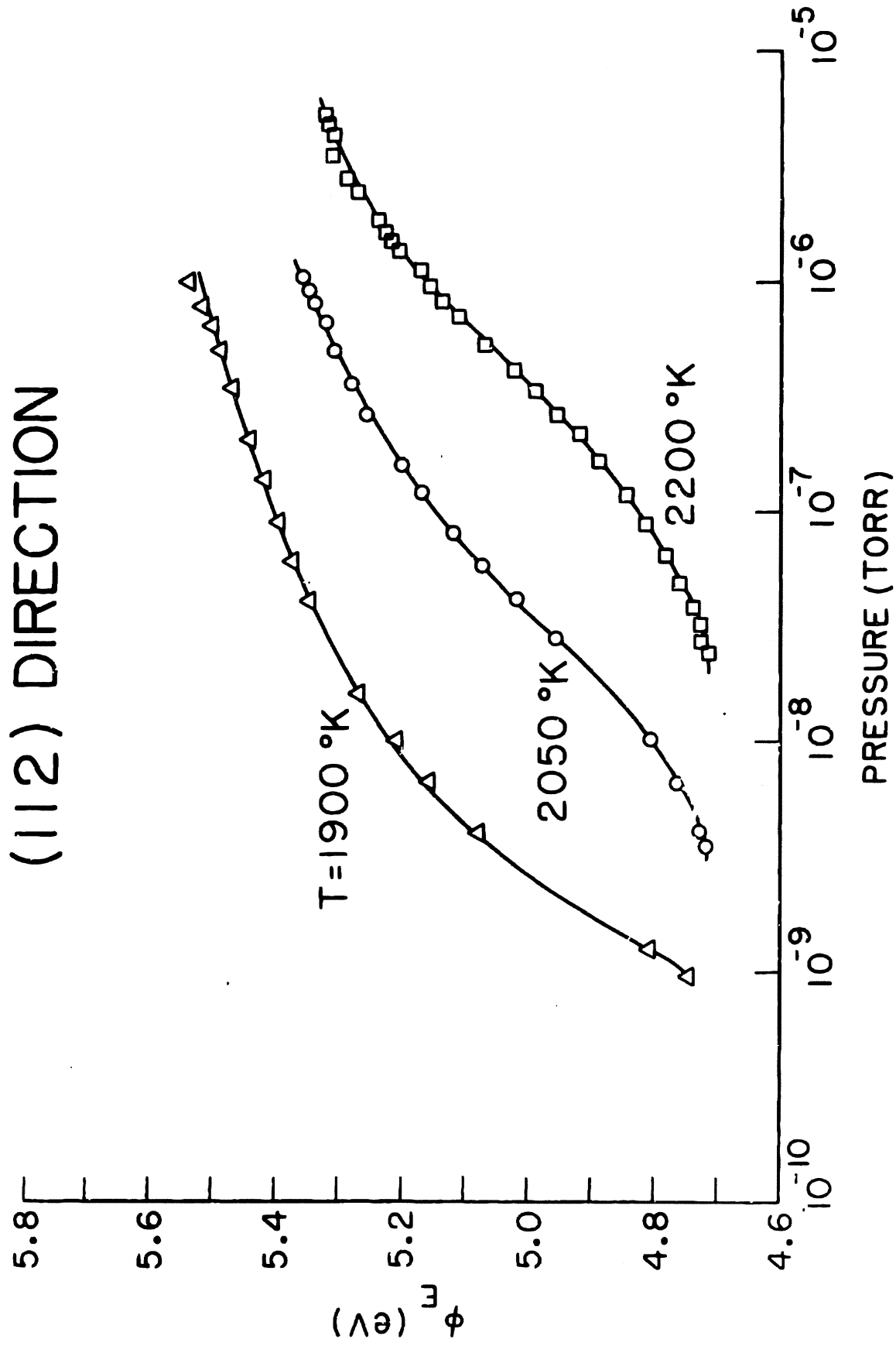


Fig. 9c Effective work function of the (112) crystallographic direction as a function of O_2 pressure and filament temperature.

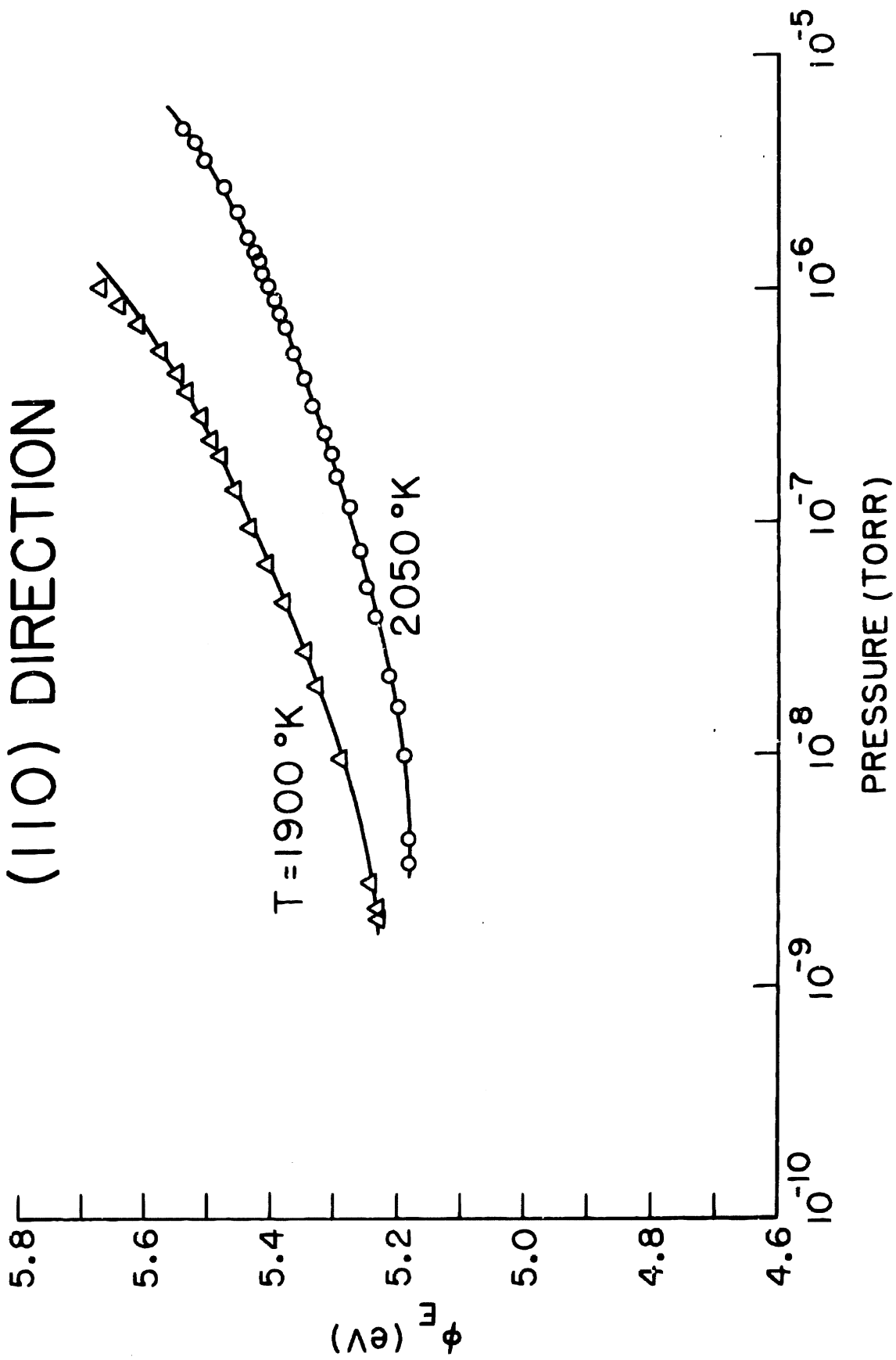


Fig. 9d Effective work function of the (110) crystallographic direction as a function of O_2 pressure and filament temperature.

the pressure of the residual gases when the O_2 valve is closed. Hence the pressure readings are the sum of the O_2 pressure and the pressure of the unknown residual gases. Although this introduces an uncertainty in the low-pressure data, this effect becomes negligible at higher pressures.

Notice that the low-pressure limiting values of ϕ_E shown in Fig. 9 are not the same for all filament temperatures. This result is to be expected if ϕ_E depends on temperature, if S is not measured accurately, or if the pre-exponential factor appearing in the Richardson equation is not 120 as assumed.

Since the O_2 coverage, θ , has not been measured in this experiment, we are unable to construct plots of ϕ_E versus θ . As an alternative, it is of interest to determine if the parameter which is useful for correlating thermionic data for alkali metals¹⁷ will also be successful for oxygen. The parameter is T/T_R , where T is the substrate (i.e., filament) temperature and T_R is the saturation temperature corresponding to the particular operating pressure of the gaseous adsorbate. The effective saturation temperatures, T_R^* , employed in Fig. 10 are computed from the following empirical expression which accurately describes data reported by Honig and Hook¹⁸ for the vapor pressure of oxygen:

$$\log_{10} P = 9.25 - \frac{486.45}{T_R^*} \quad (2)$$

Since the reciprocal of T/T_R^* may be considered as a measure of the coverage, it follows that ϕ_E should approach the clean surface value as T/T_R^* increases.

The correlation shown in Fig. 10 is surprisingly good. The scatter appearing at high values of T/T_R^* may be caused by the factors discussed previously in connection with the data of Fig. 9. The comparison of the different crystallographic directions shown in Fig. 11 is based on curves drawn through the data points of Fig. 10.

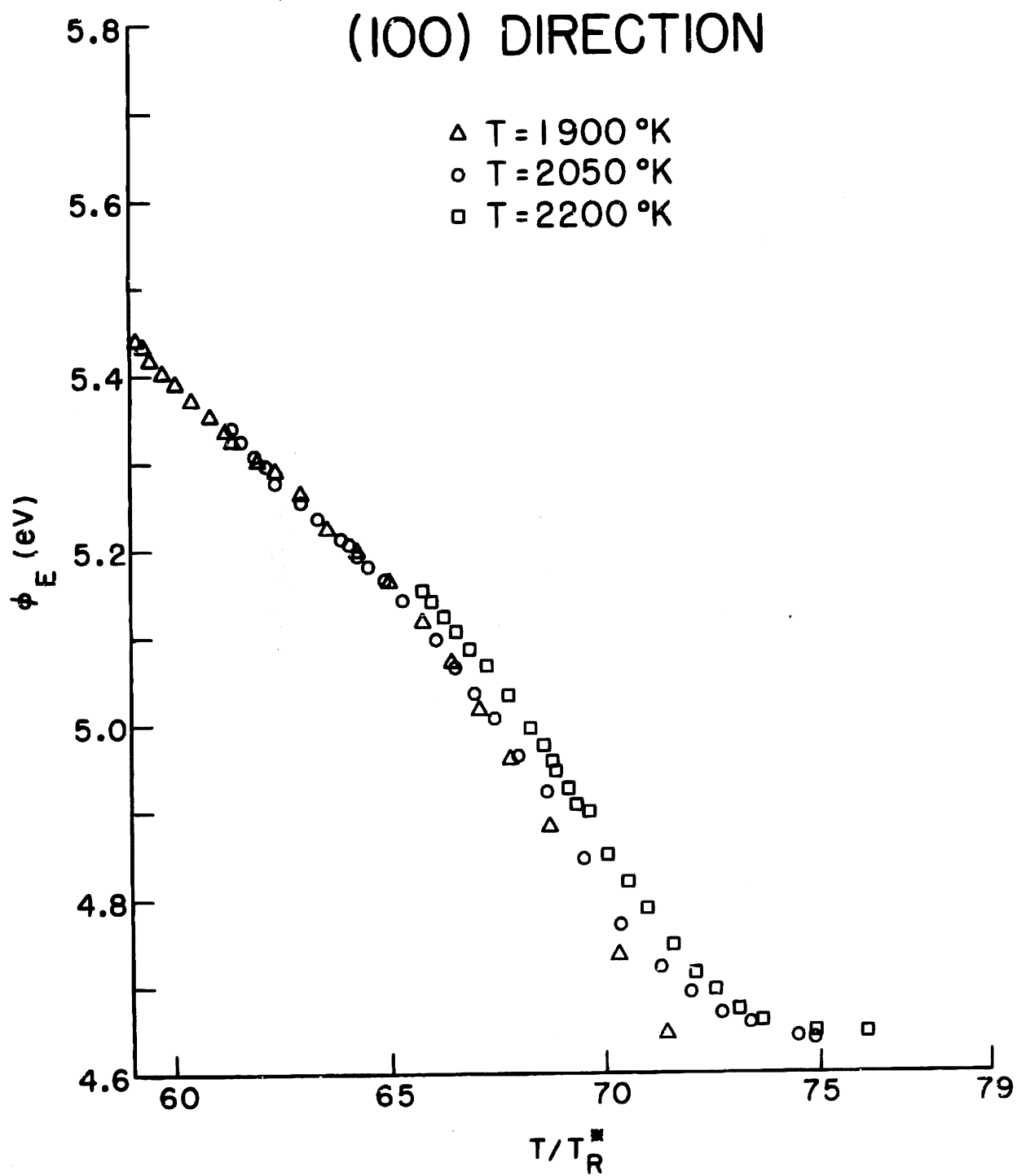


Fig. 10a Effective work function of the (100) crystallographic direction as a function of T/T_R .

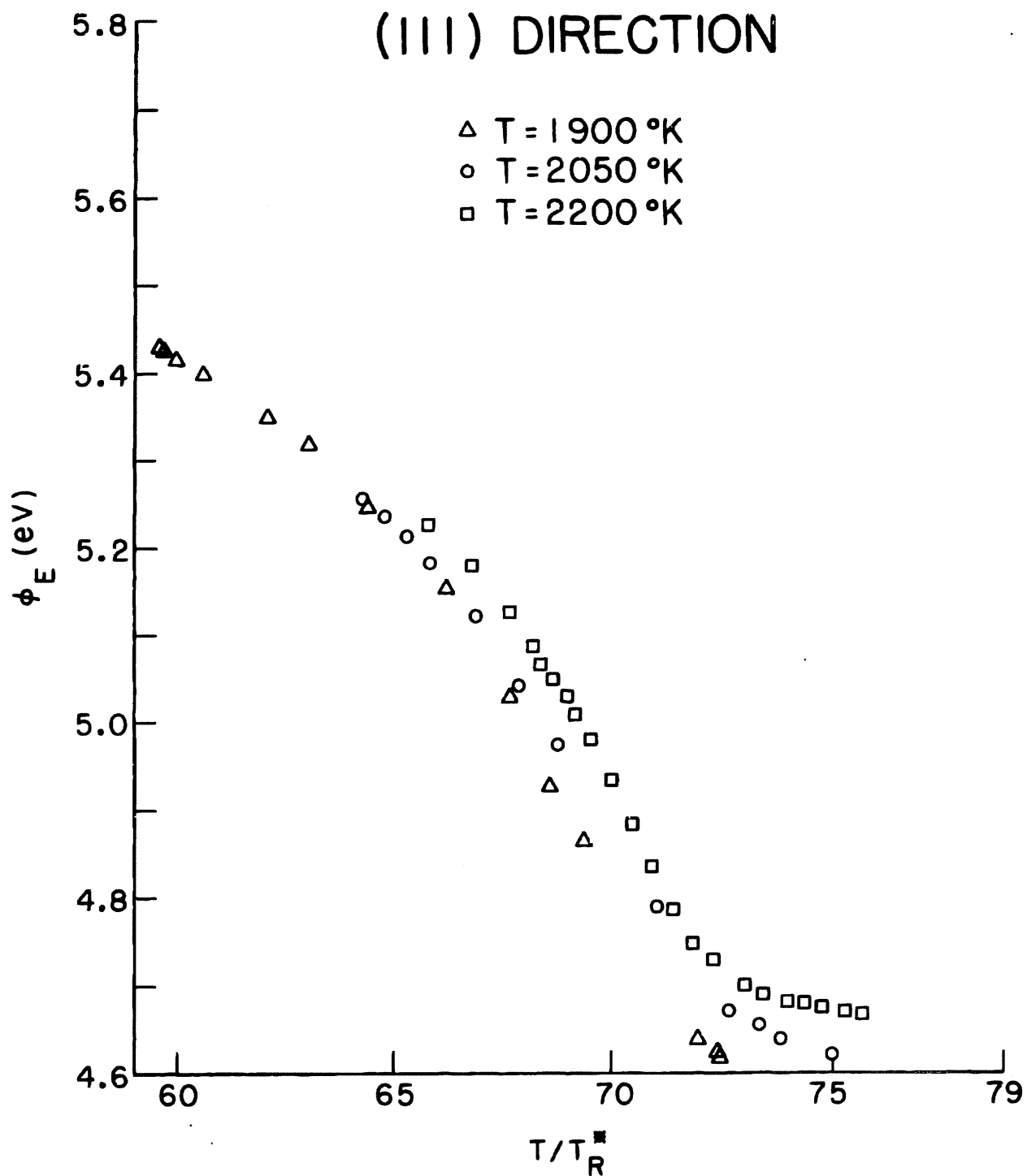


Fig. 10b Effective work function of the (111) crystallographic direction as a function of T/T_R^* .

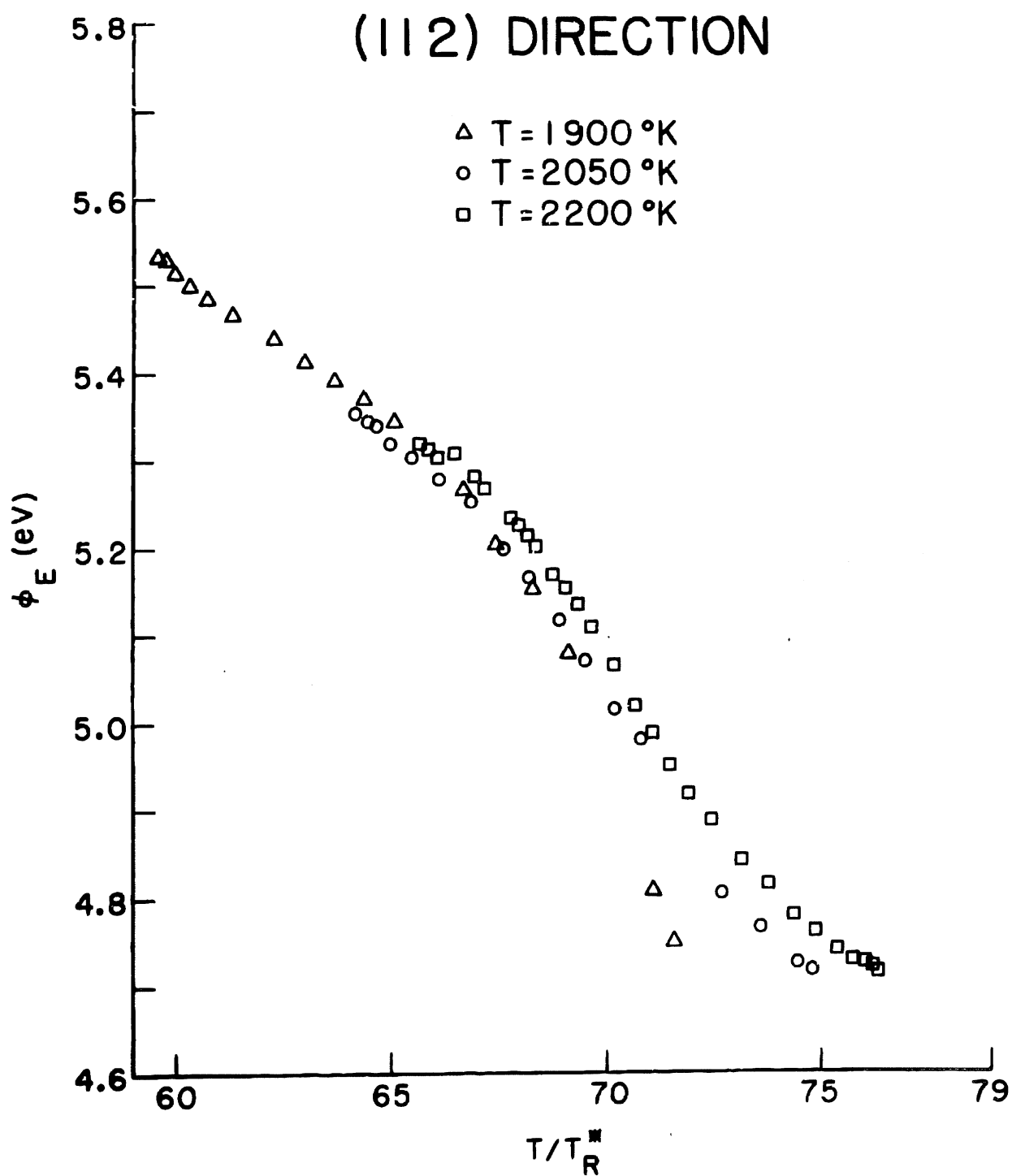


Fig. 10c Effective work function of the (112) crystallographic direction as a function of T/T_R^* .

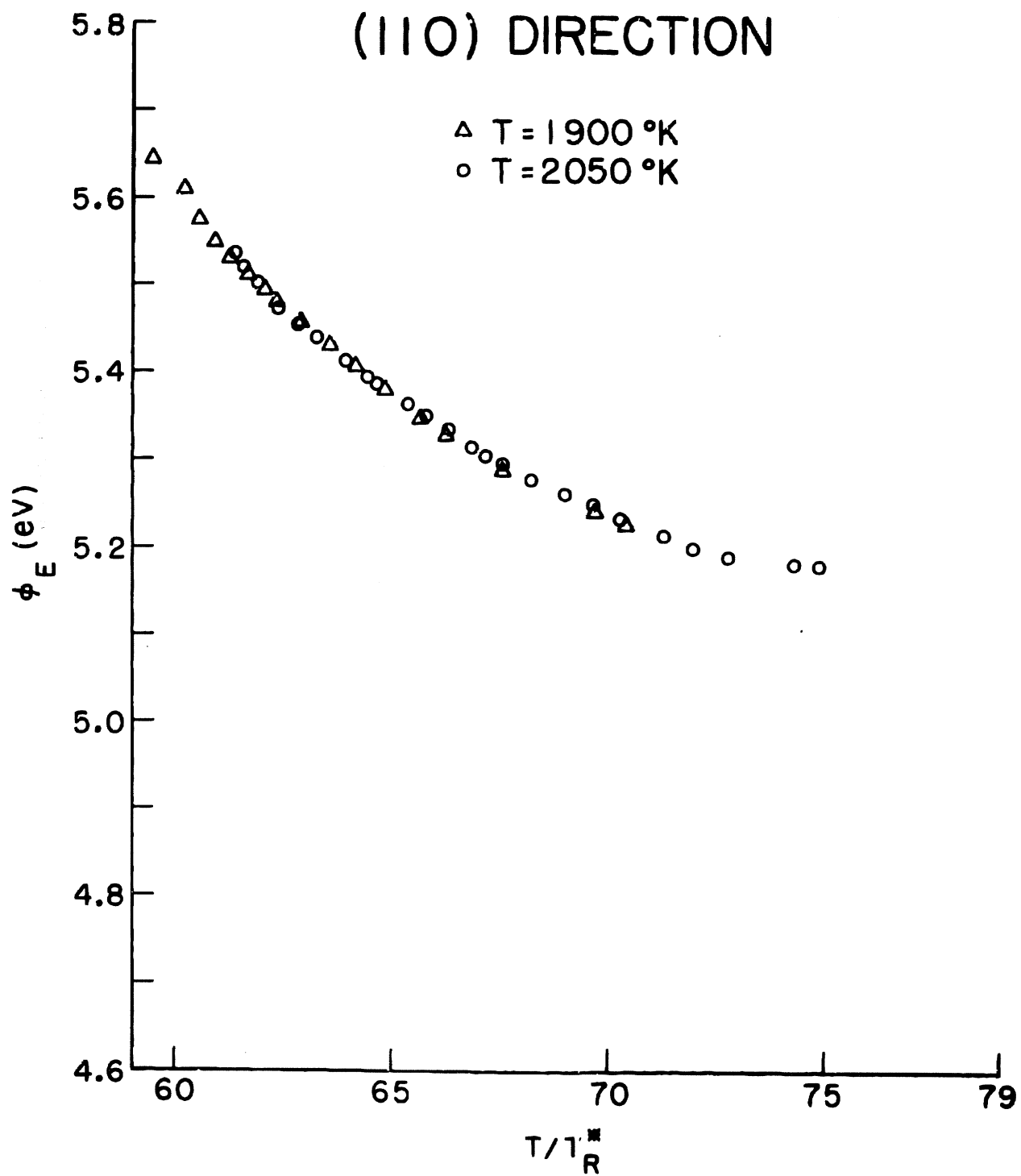


Fig. 10d Effective work function of the (110) crystallographic direction as a function of T/T_R^* .

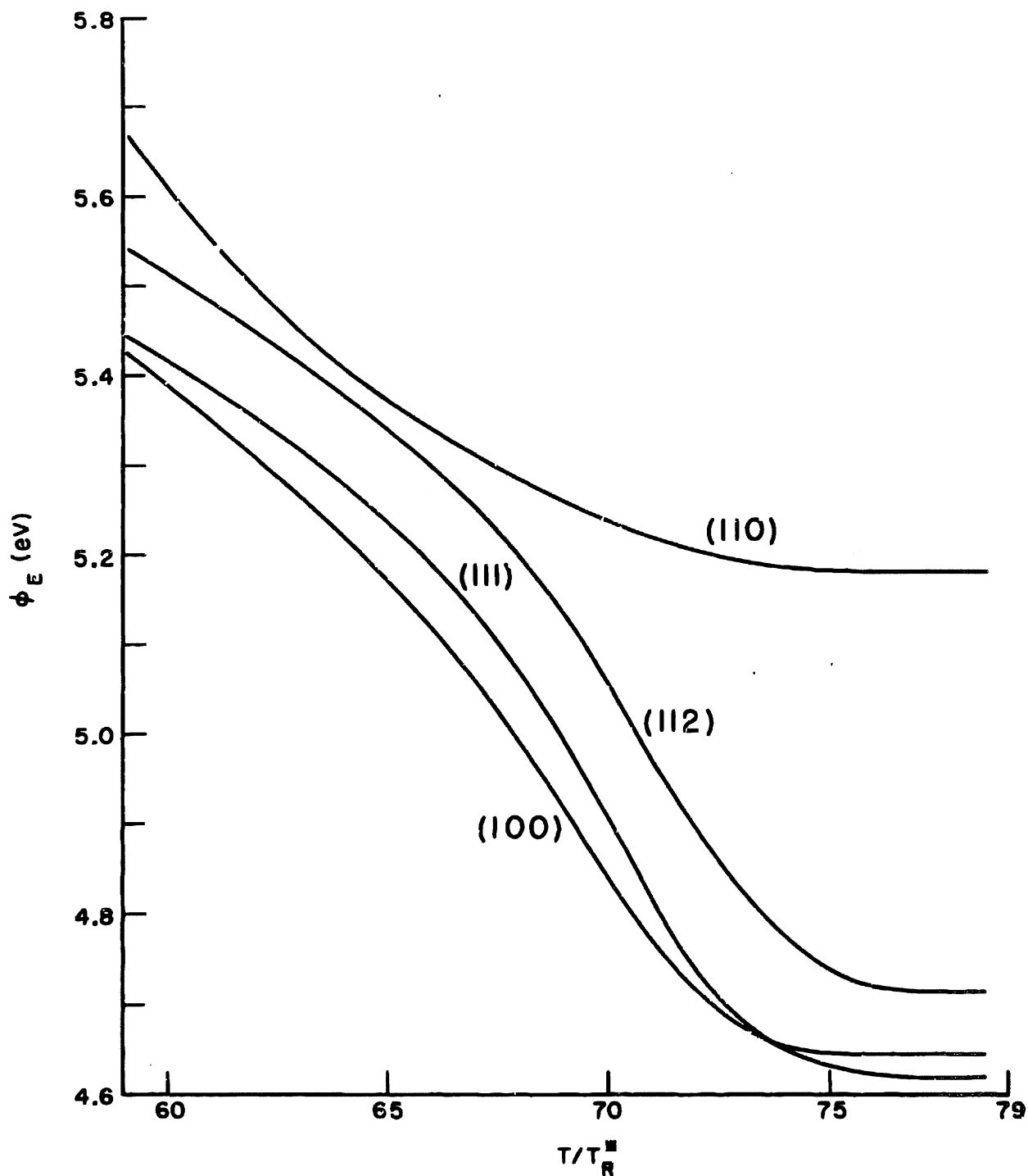


Fig. 11 Comparison of the average experimental results for O_2 on W; ϕ_E vs T/T_R^* for the (100), (111), (112), and (110) crystallographic directions.

V. RESULTS: DESORPTION ENERGY FOR O₂ ON W

The desorption energy was determined by measuring the time rate of change of the emission current when the O₂ pressure is suddenly decreased by opening the PS valve. Starting from an initial value of 1×10^{-6} Torr, the pressure drops to 1×10^{-7} within 0.6 seconds and attains a value of 1×10^{-8} within 100 seconds.

A typical example of the experimental data is presented in Fig. 12. The measured emission current, I , has been normalized with respect to I_0 , the bare-surface value. Notice that the curves for the (100) and (111) directions cross one another in Fig. 12, as well as in Fig. 11.

To enable us to compute a desorption energy from the emission data shown in Fig. 12, we must relate the effective work function, ϕ , to the O₂ coverage, θ . Since the exact form of this relation is not known at present, we are forced to use the common assumption that ϕ may be represented by the first two terms of a Taylor series expansion about the point of zero coverage. That is,

$$\phi = \phi_0 + \frac{d\phi}{d\theta} \theta, \quad (3)$$

where ϕ is the effective work function corresponding to coverage θ , and ϕ_0 is the effective work function of the bare surface ($\theta=0$). By evaluating $\frac{d\phi}{d\theta}$ at an arbitrary reference point of $\theta = \theta_I$ and $\phi = \phi_I$, Eq. (3) may be expressed as

$$\phi = \phi_0 + \frac{\phi_I - \phi_0}{\theta_I} \theta. \quad (4)$$

Hence,

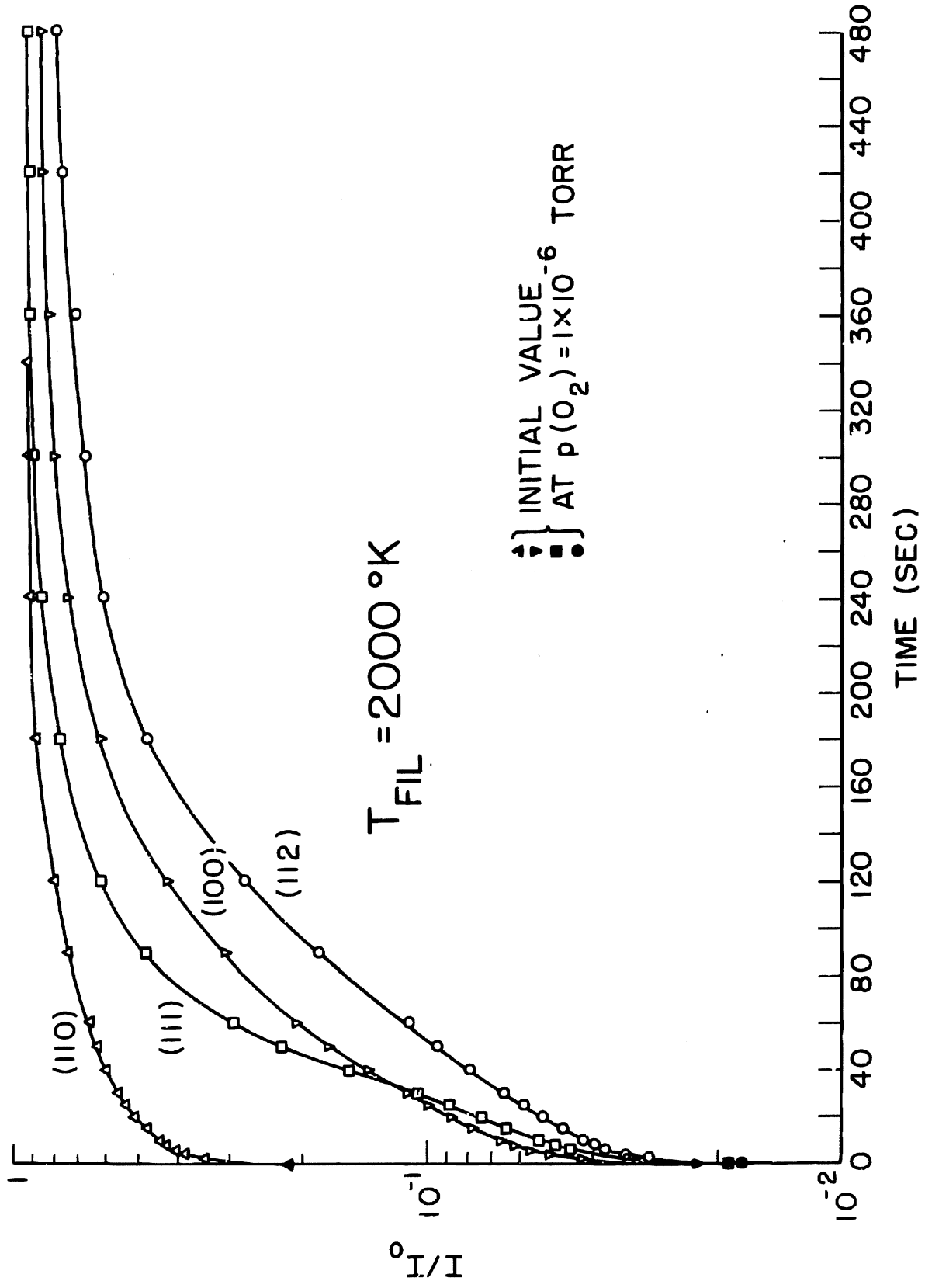


Fig. 12 Typical data obtained in desorption study.

$$\frac{\theta}{\theta_I} = \frac{\phi - \phi_0}{\phi_I - \phi_0} \quad (5)$$

From Eq. (1), the effective work function is given by

$$\phi = kT(\ln 120 ST^2 - \ln I). \quad (6)$$

This may be substituted into Eq. (5) to obtain

$$\frac{\theta}{\theta_I} = \frac{\ln I_0 - \ln I}{\ln I_0 - \ln I_I}, \quad (7)$$

where the filament temperature is the same for the three emission currents.

We shall assume here that the desorption of O_2 from W is a first-order process. (This assumption is discussed in more detail in reference 19.) If the flux of oxygen molecules upon the filament is stopped suddenly by opening the PS valve at time $t = 0$, the coverage will decrease from the initial value, θ_I , according to

$$\theta = \theta_I \exp\left[-\frac{t}{\tau}\right], \quad (8)$$

where τ is the characteristic adsorption time. If the coverage is θ_I at time t_I , then

$$\frac{\theta}{\theta_I} = \frac{\theta_I \exp(-t/\tau)}{\theta_I \exp(-t_I/\tau)} = \exp\left[-\frac{t-t_I}{\tau}\right] \quad (9)$$

or,

$$\tau = \frac{t_I - t}{\ln(\theta/\theta_I)}. \quad (10)$$

Substituting Eq. (7) for θ/θ_I , we obtain

$$\tau = (t_I - t) \left[\ln \left(\frac{\ln I_0 - \ln I}{\ln I_0 - \ln I_I} \right) \right]^{-1} \quad (11)$$

Hence, τ may be calculated from measurements of I and I_I at times t and t_I , respectively. Notice that this method of determining τ does not require knowledge of the values of θ or θ_I .

The relationship between τ and E , the desorption energy, is assumed to be

$$\tau = \tau_0 \exp \left(\frac{E}{kT} \right) \quad (12)$$

or

$$\ln \tau = \ln \tau_0 + \frac{E}{kT} \quad (13)$$

where, for first-order desorption processes, τ_0 is of the same order of magnitude as the period of vibration of an adsorbed atom.¹⁹ If τ is computed from Eq. (11) using experimental data obtained at various values of T , we may determine E and $\ln \tau_0$ from the slope and intercept, respectively, of the plot of $\ln \tau$ versus $(kT)^{-1}$.

Presented in Table I are values of τ calculated from experimental data similar to those shown in Fig. 12. Since the temperature range is not sufficient for proper use of the graphical technique described in the preceding paragraph, we have computed E from Eq. (13) by assuming that τ_0 equals 1×10^{-13} seconds. This assumption is discussed in Section VI. As shown in Table I, the magnitude of E is essentially independent of the crystallographic direction. The average value of E is 5.9 eV.

Table I. Results for the desorption of O₂ from W.

T (°K)	(112) direction		(100) direction		(111) direction		(110) direction	
	τ (sec)	E (eV)	τ (sec)	E (eV)	τ (sec)	E (eV)	τ (sec)	E (eV)
2000	159.9	6.07	140.4	6.05	85.0	5.96	96.3	5.99
2050	52.8	6.03	41.2	5.99	32.3	5.94	28.6	5.92
2100	20.8	6.01	12.9	5.92	11.4	5.90	9.0	5.86
2150	6.8	5.94	4.8	5.88	4.2	5.86	2.7	5.77

VI. DISCUSSION OF RESULTS

The effect of O_2 on the thermionic emission from W was first studied by Kingdon,²⁰ in 1924. A similar investigation was performed in greater detail by Johnson and Vick,²¹ in 1937. Polycrystalline tungsten filaments were employed in both experiments, and the O_2 pressure was not accurately measured.

Using the contact potential method, Langmuir and Kingdon²² measured work-function changes for O_2 on W which were much smaller than those computed from the thermionic data of Kingdon.²⁰ Reimann²³ repeated the contact-potential measurements and obtained a maximum contact-potential change of 1.7 eV for O_2 on W at room temperature. This value is in good agreement with that computed from Kingdon's data, and it has been verified in subsequent investigations both with the field emission microscope and the contact potential method.²⁴ A detailed study of the change in contact potential with increasing O_2 coverage on polycrystalline W has been performed by Bosworth and Rideal.²⁵

Since the results of the present study are, to the best of our knowledge, the first thermionic measurements of the effect of O_2 on the work function of a single-crystal substrate, we have no standard of comparison. Becker and Brandes⁵ have, however, used the field emission microscope to investigate the effect of O_2 on various crystallographic planes of W. The general characteristics of our results agree qualitatively with those of Becker and Brandes. Quantitative agreement is not expected because of the significant differences in the experimental techniques. Mueller,²⁶ Gomer and Hulm,⁴ and George and Stier²⁷ have also used the field emission microscope to study O_2 on W.

As seen in Fig. 11, the maximum work-function change determined from the present data is ~ 0.83 eV. This value is

less than that measured in contact-potential studies because the filament temperature is sufficiently high to reduce the O_2 coverage below the maximum possible value. As inferred in the selection of T/T_R^* as the correlation parameter, the coverage increases with increasing pressure and decreasing filament temperature. It is expected that, for the range of pressures and temperatures used here, the surface coverage does not exceed one monolayer of atomic oxygen.^{5,13}

Although the structure of O_2 on W is not completely understood, there is evidence that adsorption and surface rearrangement is greatest on crystallographic planes having an open lattice structure.¹⁴ This provides a possible explanation for the fact that the work function of the (110) direction is not affected by O_2 as markedly as the other crystallographic directions (Fig. 11). (We prefer to use the term "crystallographic direction" instead of "crystallographic plane" because the exact surface structure of the tungsten filament is not known.)

Since it is known that the presence of carbon impurities in tungsten may affect both the thermionic and adsorption properties of the specimen,²⁸ we attempted to remove these impurities from the filament by employing the process recommended by Becker et al.¹³ Assuming that the process is effective, we conclude from the data that the initial concentration of C was sufficiently low to have little influence on the work function. It is of interest to note that there is some evidence that minute traces of C on W may cause the desorption energy of O_2 to increase.²⁸

Although the desorption of O_2 from W has been considered by several different investigators,^{5,21,25,29} the process is not understood completely because the agreement of the experimental data is unsatisfactory. Desorption energies ranging from 4 to 7 eV have been reported, and it is not known with certainty if oxygen desorbs as atoms or as molecules.^{13,19}

The problem is complicated by the fact that various oxides also desorb from the surface as a result of the reaction of O_2 with tungsten^{13,30} and with the carbon impurities.¹³

The experimental method used here to determine the desorption energy of O_2 on W differs from that which is normally employed. The average value of 5.9 eV is, however, in fair agreement with the values 6.4 and 6.7 eV reported by Johnson and Vick²¹ and by Bosworth and Rideal,²⁵ respectively. Because the temperature range of our data is narrow, we have assumed that the desorption is a first-order process with τ_0 equal to 1×10^{-13} seconds. This assumption is based on the results of Johnson and Vick.²¹

As shown in Table I, it appears that the desorption energy, E , is essentially the same for (100), (111), (112), and (110) crystallographic directions. We believe, however, that this apparent result is false because the physical model employed in Section V does not account for the possibility that surface migration of adsorbed oxygen atoms may be so rapid that the majority of the desorption occurs from the crystallographic surface having the smallest desorption energy. If surface migration is dominant, the experimental values of E reported here and elsewhere are representative of the minimum values of the specific specimens. We conclude, therefore, that the method used by Becker and Brandes⁵ to estimate the dependence of E on crystallographic structure may be invalid.

It is possible that surface migration may also have a significant effect on the thermionic measurements described in Section IV. For example, the O_2 coverage on a specific crystallographic surface for a given temperature and pressure will depend upon the desorption energies of the adjacent crystallographic patches if the migration rate is much larger than the desorption rate. Hence the experimental results presented here may not apply to tungsten specimens having different patch sizes and relative orientations.

REFERENCES

1. I. Langmuir and K. H. Kingdon, *Phys. Rev.* 23, 112 (1923).
2. J. M. Houston and H. F. Webster, in *Advances in Electronics and Electron Physics*, Vol. 16, p. 167, (L. Marton, editor), Academic Press (1962).
3. For example, see: R. L. Amodt, L. J. Brown, and B. D. Nichols, *J. Appl. Phys.* 33, 2080 (1962); L. S. Swanson, R. W. Strayer, and F. M. Charbonnier, Report on Twenty-Fourth Annual Conference on Physical Electronics, 120, (1964); C. H. Skeen, *J. Appl. Phys.* 36, 84 (1965); also see the Reports on the 1964 and 1965 Thermionic Conversion Specialist Conferences.
4. R. Gomer and J. K. Hulm, *J. Chem. Phys.* 27, 1363 (1957).
5. J. A. Becker and R. G. Brandes, *J. Chem. Phys.* 23, 1323 (1955).
6. J. L. Coggins and R. E. Stickney, Report on the Twenty-Fifth Annual Conference on Physical Electronics, 67 (1965).
7. C. S. Robinson, *J. Appl. Phys.* 13, 647 (1942).
8. G. F. Smith, *Phys. Rev.* 94, 295 (1954).
9. R. J. Zollweg, *J. Appl. Phys.* 34, 2590 (1963).
10. M. H. Nichols, *Phys. Rev.* 57, 297 (1940).
11. E. A. Coomes and F. E. Girouard, Report on the Thermionic Conversion Specialist Conference, 47 (1964).
12. J. L. Coggins, Ph.D. Thesis, Dept. of Mechanical Engineering, M.I.T., 1965.
13. J. A. Becker, E. J. Becker, and R. G. Brandes, *J. Appl. Phys.* 32, 411 (1961).
14. J. A. Becker, *Advances in Catalysis* 7, 135 (1955); R. Gomer, *Advances in Catalysis* 7, 93 (1955); N. J. Taylor, *Surface Sci.* 2, 544 (1964); J. Anderson and W. E. Danforth, *J. Franklin Inst.* 279, 160 (1965).

15. H. A. Jones and I. Langmuir, G. E. Rev. 30, 310, 354, 408 (1927).
16. S. Dushman, Scientific Foundations of Vacuum Technique, John Wiley & Sons, Inc. (2nd Edition, 1962).
17. N. S. Rasor and C. Warner, J. Appl. Phys. 35, 2589 (1964). (For a thermodynamic treatment, see E. N. Carabateas, J. Appl. Phys. 33, 2698 (1962).)
18. R. E. Honig and H. O. Hook, R.C.A. Review 21, 360 (1960).
19. G. Ehrlich, Structure and Properties of Thin Films, pp. 423-475 (edited by C.A. Neugebauer, J. B. Newkirk, and D. A. Vermilyea), John Wiley & Sons, Inc., New York (1959).
20. K. H. Kingdon, Phys. Rev. 24, 510 (1924).
21. M. C. Johnson and F. A. Vick, Proc. Roy. Soc. A151, 308 (1935).
22. I. Langmuir and K. H. Kingdon, Phys. Rev. 34, 129 (1929).
23. A. L. Reimann, Phil. Mag. 20, 594 (1935).
24. The results of these investigations have been summarized by R. V. Culver and F. C. Tompkins, Advances in Catalysis 11, 67, Academic Press, New York, 1959.
25. R. C. L. Bosworth and E. K. Rideal, Physica 4, 925 (1937); also see R. C. L. Bosworth, Proc. Roy. Soc. (New South Wales) 79, 190 (1946).
26. E. W. Mueller, Ergeb. exakt. Naturw. 29, 290 (1953).
27. T. H. George and P. M. Stier, J. Chem. Phys. 37, 1935 (1962).
28. J. A. Becker, Advances in Catalysis 7, 135 (1955).
29. I. Langmuir and D. S. Villars, J. Am. Chem. Soc. 53, 486 (1931)
30. J. B. Berkowitz-Mattuck, A. Buchler, J. L. Engelke, and S. N. Goldstein, J. Chem. Phys. 39, 2722 (1963).